Surface Science 603 (2009) 1262–1269

Contents lists available at ScienceDirect

Surface Science

journal homepage: www.elsevier.com/locate/susc

CO interaction with Au atoms adsorbed on terrace, edge and corner sites of the MgO(1 0 0) surface. Electronic structure and vibrational analysis from DFT

Ricardo M. Ferullo [a,b,*], Silvia A. Fuente [a], Patricia G. Belelli [a], Norberto J. Castellani [a]

[a] Grupo de Materiales y Sistemas Catalíticos, Departamento de Física, Universidad Nacional del Sur, Av. Alem 1253, 8000 Bahía Blanca, Argentina
[b] Departamento de Química, Universidad Nacional del Sur, Av. Alem 1253, 8000 Bahía Blanca, Argentina

ARTICLE INFO

Article history:
Received 23 December 2008
Accepted for publication 15 March 2009
Available online 24 March 2009

Keywords:
Au/MgO
Model catalysts
CO adsorption
DFT
Cluster model

ABSTRACT

The interaction of CO with Au atoms adsorbed on terrace and low-coordinates sites (edge and corner) of the MgO(1 0 0) surface was studied using the density functional theory (DFT) in combination with embedded cluster models. Surface anionic (O^{2-}) and neutral oxygen vacancy (F_s) sites were considered. In all the cases, the CO stretching frequencies are shifted with respect to free CO with values between −232 and −358 cm^{-1}. In particular, the values for Au on F_s at edge and corner are shifted to higher stretching frequencies by 100 and 59 cm^{-1}, respectively, with respect to the value on a perfect MgO(1 0 0) surface. This result is in agreement with recent scanning tunneling microscopy and infrared spectroscopy experiments where a corresponding shift of 70 cm^{-1} was observed by comparing the measurements on perfect and O-deficient MgO(1 0 0) surfaces. However, these results are different than expected because Au atoms on F_s centers are negatively charged and, therefore, according to the generally accepted scheme the CO frequency should be red-shifted with respect to the adsorption on anionic five-coordinated site where the Au atom is essentially neutral. The following picture emerges from the present results: the single occupied HOMO(α) of Au atom on F_s at low-coordinated sites consists in two lobes extended sideward the Au atom. For symmetry reasons, this MO overlaps efficiently with the $2\pi^*$ MO of CO. This bonding contribution to the Au–CO link is counteracted by a Pauli repulsion between the 5σ MO of CO and more internal orbitals (the HOMO-1(α) and the HOMO(β)) centered on Au. In consequence, CO is forced to vibrate against a region with a high electron density. This is the so-called "wall effect" which by itself contributes to higher CO frequency values.

1. Introduction

Nowadays it is possible to prepare model catalysts consisting in size-selected metal aggregates deposited on well-defined surfaces. Surprisingly, it was observed that already supported single atoms are chemically active for several reactions [1]. The electronic structure of the metal particles is directly affected by the surface defects where they are anchored, which in turn determine their catalytic activity [2].

By means of infrared (IR) spectroscopy, CO stretching frequency is usually used as a reporter of the nature of the adsorbed metal aggregates [3,4]. This is because the CO vibrational frequency is very sensitive to small changes in the electron density of the metal adsorption site. As a general trend, CO frequency shifts to higher values with respect to free CO on positively charged particles (blue-shift) and to lower frequencies on negatively charged particles (red-shift). On neutral particles the frequencies are often red-shifted but to a lesser extent than on negative clusters. Although several factors are responsible for the CO frequency shifts [5], they are usually interpreted in terms of the donation/backdonation mechanism. In this scheme, the 5σ (the HOMO) and $2\pi^*$ (the LUMO) orbitals of CO interacts with the metal particle. While the former is generally considered as weakly antibonding, the latter is strongly antibonding. With positively metal centers, CO acts as a Lewis base by means of the donation from the 5σ orbital to empty orbitals of the metal. In this case, the backdonation from the metal to the $2\pi^*$ orbital is very low. As a result, the CO frequency shifts to higher values. With negative particles, the donation from 5σ is negligible but the backdonation to $2\pi^*$ is relevant yielding a weakening of the C–O bond and a decreasing of C–O frequency values.

In particular, in gold catalysts supported on a variety of oxides the following spectral ranges were reported: (i) 2124/2175 cm^{-1} assigned to positively charged Au particles; (ii) 2088/2136 cm^{-1} assigned to neutral particles; and (iii) 2000/2070 cm^{-1} assigned to negatively charged particles. The corresponding frequency shifts with respect to free CO are −19/+32 cm^{-1}, −55/−7 cm^{-1} and −143/−73 cm^{-1}, respectively [4,6].

* Corresponding author. Address: Grupo de Materiales y Sistemas Catalíticos, Departamento de Física, Universidad Nacional del Sur, Av. Alem 1253, 8000 Bahía Blanca, Argentina. Tel.: +54 291 4595141; fax: +54 291 4595142.
E-mail address: caferull@criba.edu.ar (R.M. Ferullo).

0039-6028/$ - see front matter © 2009 Elsevier B.V. All rights reserved.
doi:10.1016/j.susc.2009.03.015

Recently, Au/MgO model catalysts were investigated at ultra-high vacuum conditions by Sterrer et al. [6] by using scanning tunneling spectroscopy (STM) and electron paramagnetic resonance (EPR). On the perfect MgO(1 0 0) surface, gold aggregates interact with regular anionic sites. Upon CO adsorption, a signal at 2120 cm^{-1} was detected which was attributed to neutral Au clusters. This value corresponds to a shift of −23 cm^{-1}, falling into the range assigned to neutral metal particles. Later, the same procedure was applied to a defective MgO(1 0 0) surface, in which O-vacancies were created by electronic bombardment. These defects corresponds mainly to F_s o F_s^+ centers, generated by the removal of a neutral O atom and an O^- anion, respectively. As a consequence, at F_s (F_s^+) sites two (one) electrons are trapped inside the cavity. In this situation, upon CO adsorption a broad band at 2070 cm^{-1} was observed which corresponds to a shift of −73 cm^{-1}. This band was assigned to negative Au clusters. Indeed, when gold particles interact with F_s or F_s^+ centers a charge transfer occurs from the cavity to the metal [6–9]. Besides, the CO frequency shift is very sensible to the size particle; it decreases as the size increases owing to a higher charge dilution. As a consequence, a lower backdonation to CO is produced with the concomitant lower red-shift. This phenomenon can then explain the observed large band broadening.

At the same time, the above mentioned experimental group performed a similar study but only considering Au atoms [10]. Combined analyses using EPR and STM show that while on perfect MgO(1 0 0) surface the metal atoms adsorb on regular five-coordinated anionic sites, on the defective surface they are mainly located on O-vacancies at topological defects such as steps, corners or kinks. The CO frequency values present signals at 1853 cm^{-1} for Au atom deposited on the perfect MgO(1 0 0) surface and at 1923 cm^{-1} for Au atom on O-deficient samples. These values are red-shifted by −290 and −220 cm^{-1}, respectively, and are much below any other reported value for supported Au catalysts. On the other hand, for Au atoms interacting with electron-rich defects (such us F_s or F_s^+ centers) one should expect a higher red-shift than on a regular anionic sites because in the former case the negative charged Au atom should provide a large amount of charge to the $2\pi^*$ orbital. But, very surprisingly, the CO frequency is blue-shifted by 70 cm^{-1} with respect to the adsorption on a regular anionic site.

From theoretical calculations the following picture was suggested [10]: on a perfect MgO(1 0 0) surface, the adsorbed AuCO is essentially neutral. The presence of CO induces a net electron transfer into the $2\pi^*$ antibonding orbital resulting in a Au^+–CO^- complex. However, according to this interpretation, such as charge transfer is not present on F_s centers. In this way, the electron-withdrawing capability of the AuCO species would be stronger on five-coordinated oxygen anions than at F_s centers at MgO terrace. On the other hand, it has been recently discovered by means of theoretical DFT approaches that negative charged Au atoms can be produced when they are deposited on free-defect ultrathin MgO on Mo(1 0 0) or on Ag(1 0 0) [11]. In these systems the electrons flow by tunneling from the metal (Ag or Mo) to the Au atom. The calculations show that when a CO molecule is adsorbed on this negative charged Au atom its frequency is red-shifted by −186 cm^{-1} with respect to free CO. It was suggested that a Pauli repulsion should be present between Au^- and the 5σ of CO, yielding to a rather long Au–CO distance and a relatively low charge transfer from Au to $2\pi^*$ MO of CO.

The adsorption of Au atoms on MgO(1 0 0) surface have been thoroughly studied in the past, mainly by using periodic supercell approaches [7,12–16]. However, the deposition on topological defects, such as steps, edges and corners, has received much less attention [7,17]. These low-coordinated sites are found to be more reactive than terrace on both oxide and metal surfaces [18–20]. Besides, as it was already mentioned, STM images show that Au atoms interact with O-vacancies located on this type of topological defects. The main objective of this work is to investigate the origin of the unexpected lower red-shift of the CO frequency when this molecule is adsorbed on a negatively charged Au atom in comparison with the adsorption on a neutral Au atom. For that purpose anionic sites and neutral O-vacancies (F_s) located at terrace, edge and corner sites of the MgO(1 0 0) surface were considered.

2. Computational details

Density functional theory (DFT) molecular orbital calculations were carried out using the gradient corrected Becke's three parameters hybrid exchange functional in combination with the correlation functional of Lee, Yang and Parr (B3LYP) [21]. This method was widely used in the past to study adsorption processes yielding reliable results both on oxides and metal clusters. All the calculations have been performed using the Gaussian-03 program package [22].

The terrace site at MgO(1 0 0) surface was represented by a cluster of 26 atoms, $Mg_{13}O_{13}$, consisting of two layers (first layer: Mg_4O_9; second layer: Mg_9O_4). To take into account the Madelung field due to the rest of the extended surface, the cluster was embedded in an array of ±2 point charges. Moreover, the positive point charges at the interface were replaced by effective core potentials (ECP) corresponding to Mg^{2+} to account for the finite size of the cations and to avoid spurious charge polarization. The $Mg_{13}O_{13}$(Mg-ECP)$_{16}$ is represented in Fig. 1a. This methodology was widely used previously for the study of both bulk and surface properties giving results which are in good agreement with those obtained by periodic calculations [23–25]. For edge and corner sites we used a similar modelling by means of the $Mg_{12}O_{12}$(Mg-ECP)$_{14}$ and $Mg_{10}O_{10}$(Mg-ECP)$_9$ clusters, respectively (Fig. 1b and c).

The O ion which represents the adsorption site and the nearest four O neighbours (three for corner site) were described by the 6−31+G(d) basis set. This extended basis set was adopted to have a proper description of the central surface anions. The atomic orbitals of the four Mg ions (three for corner site) linked directly with the O adsorption site were described by 6−31G(d). The use of a set of polarization functions in this basis set is essential to describe the electron localization in the vacancy for clusters representing the F_s sites (see later). The rest of Mg and O ions were represented by 6−31G. The 6−31+G(d) basis set was employed for the atoms of the CO molecule. For Au, the LANL2DZ basis set was used, which describes the 19 valence $5s^25p^65d^{10}6s^1$ electrons with a [5*s*,6*p*,4*d*/3*s*,3*p*,2*d*] basis set and the one-electron interaction with the 60 core electrons with a relativistic pseudopotential [26,27]. The combination of Pople-type and LANL2DZ-type basis sets was used previously by Giordano et al. [25] to study the AuCO and AuCO/MgO systems at B3LYP level. These authors showed that the 6−311+G(d) basis for CO and LANL2DZ basis with two extra *f* functions for Au give C–O frequency shifts that are only 10% or less different than those calculated with the 6−31G(d) basis for CO and a LANL2DZ basis for Au. On the other hand, interatomic distances and adsorption energies are only 5% and 15% or less different, respectively.

During the geometrical optimization procedure the coordinates of atoms belonging to the adsorbed CO molecule and the metal particle, and those of the five oxide surface atoms closest to the Au particle (four for corner site) were fully optimized without imposing geometric constrains. On sites free of vacancies, only the adsorption on the anionic site was studied because it is well known that this is the preferred adsorption site for most transition metal atoms [28].

A neutral O vacancy was represented by eliminating an O atom to the above-described clusters (Fig. 2). In these cases, the geometrical optimization included the four Mg atoms surrounding the vacancy (three for corner site).

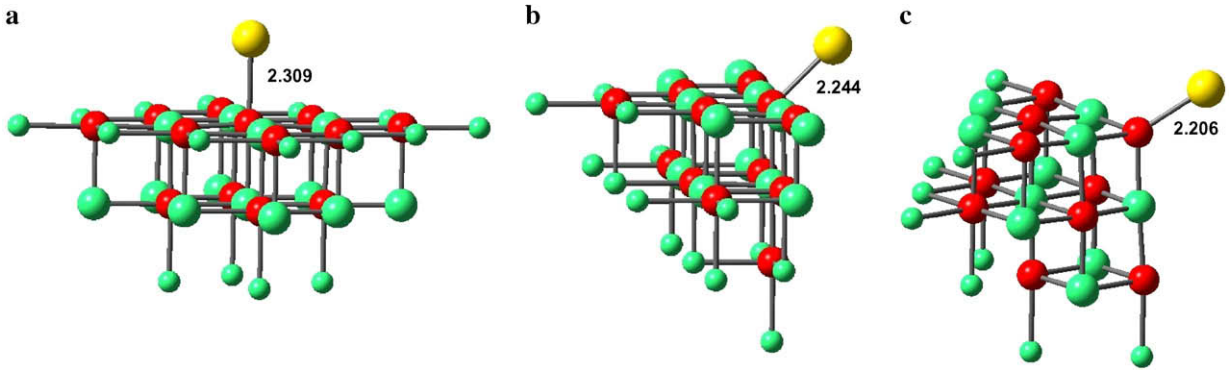

Fig. 1. Schematic representation of Au atoms deposited on anionic sites (O^{2-}): (a) terrace; (b) edge; (c) corner. Red (dark grey) spheres: oxygen atoms. Green (light grey) spheres: Mg atoms. Small green (light grey) spheres: Mg-ECPs. Large yellow (grey) spheres: Au atoms. Point charges are not shown. (For interpretation of the references to colour in this figure legend, the reader is referred to the web version of this article.)

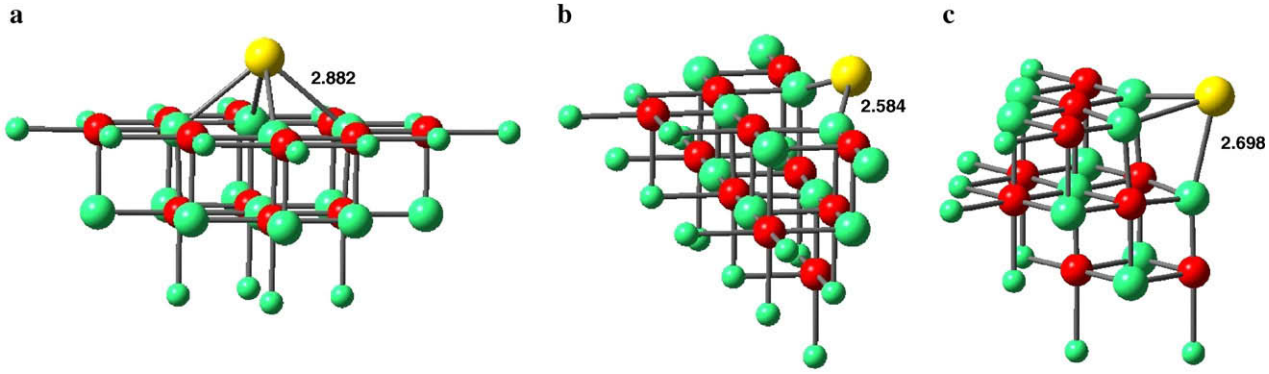

Fig. 2. Schematic representation of Au atoms deposited on F_s sites: (a) terrace; (b) edge; (c) corner. Red (dark grey) spheres: oxygen atoms. Green (light grey) spheres: Mg atoms. Small green (light grey) spheres: Mg-ECPs. Large yellow (grey) spheres: Au atoms. Point charges are not shown. (For interpretation of the references to colour in this figure legend, the reader is referred to the web version of this article.)

We define the binding energy of the Au atom on MgO as the difference between the energy of the Au/MgO system and the sum of energies for the separated fragments (MgO + Au atom at gas phase):

$$E_B(\mathrm{Au}) = -[\mathrm{E(Au/MgO, site)} - \mathrm{E(Au)} - \mathrm{E(MgO, site)}] \quad (1)$$

with site = O^{2-} or F_s at terrace, edge or corner. Similarly, we define the binding energy of CO molecule on Au/MgO as

$$E_B(\mathrm{CO}) = -[\mathrm{E(CO/Au/MgO, site)} - \mathrm{E(Au/MgO, site)} - \mathrm{E(CO)}] \quad (2)$$

In both cases, positive values correspond to exothermic processes. The binding energies were corrected by considering the basis set superposition error (BSSE), calculated according to the counter-poise correction [29].

When embedded clusters are used a key issue to consider is the cluster size dependence of the binding energies. To check this, the adsorption of a Au atom on O^{2-} at terrace site was investigated for the following Mg_nO_n clusters: Mg_5O_5(Mg-ECP)$_{12}$, $Mg_{13}O_{13}$(Mg-ECP)$_{16}$ and $Mg_{21}O_{21}$(Mg-ECP)$_{28}$. All these clusters were constructed using the above mentioned embedding technique and the same basis sets. The results show that the binding energy for the first one is about 0.15 eV greater while for the third one is nearly 0.05 eV smaller. Then, the values obtained using the second cluster can be considered sufficiently accurate to evaluate the Au–MgO interaction.

C–O vibrational frequencies are computed by determining the second derivatives of the energy with respect to the Cartesian nuclear coordinates and then transforming to mass-weighted coordinates. Our numerical accuracy for the frequency calculations is in the order of hundredth of cm^{-1}. In relation with the effect of the cluster size, our experience have shown that the stretching frequency of adsorbed CO is about 10–15 cm^{-1} lower for smaller clusters than the ones used here, and less than 10 cm^{-1} different for bigger ones.

For simplicity, anionic centers located on the different surface sites will be denoted as "terrace(O^{2-})", "edge(O^{2-})" and "corner(O^{2-})". For F_s sites we used an equivalent nomenclature, that is to say, "terrace(F_s)", "edge(F_s)" and "corner(F_s)".

The atomic net charges were calculated following the Natural Bond Orbital (NBO) scheme [30], which gives realistic values for the charge partitioning. In particular, it has been very useful for the interpretation of IR frequency shifts of NO at free and supported AuNO complex [9,31]. This method transforms a delocalized many-electron wave-function into a localized set of Lewis-type (σ and π bonds, lone pair and core) and non-Lewis-type (σ^* and π^* antibonds and Rydberg) orbitals. The interaction among orbitals belonging to these two groups is used as a measure of the electronic delocalization within a certain molecular system.

The core level binding energies (CLBE) of the C(1s) and O(1s) levels of adsorbed CO were also computed. When, for instance, the CO molecule gains electron charge upon adsorption, the core levels shift to smaller binding energies due to the increased coulombic repulsion. However, since other factors contribute to these energy shifts, CLBE are often use only as a qualitative measure of an atomic charge [32]. By convention, shifts to smaller binding energies correspond to negative values and they are indicated as $\Delta\varepsilon$(C or O, 1s).

The spin density (SD) was expressed in terms of the Mülliken population analysis. Although the NBO approach gives more reliable atomic charge values than the Mülliken scheme, the corresponding spin densities calculated from both analyses show similar trends. Here, we decided to report the Mülliken spin densities in order to compare our values with those obtained by Giordano et al. [25].

3. Results and discussion

DFT calculations on Au_1 adsorption on anionic and F_s sites of MgO(1 0 0) were previously performed by several authors using mainly periodic methods. In Table 1 we compare our results with those obtained using the following GGA functionals: PW91 [33], PBE [34] and revised-PBE (RPBE) [35]. We can see that the binding energy values obtained at our level of calculation agree fairly well with the other reported results. They are somewhat lower than those obtained using PW91 and PBE functionals, and slightly higher than those done using RPBE. On the other hand, while the binding energy difference between on anionic and F_s sites is in the range 2.17–2.28 eV for PW91, PBE and B3LYP (this work), it is lower at the RPBE level (1.84 eV).

A more detailed examination of the values at Table 1 shows that as a general trend the binding energies at RPBE level are about 20–25% smaller than using PW91 and PBE. This trend is the same as that obtained in the past for other systems. Indeed, Hammer et al. have studied the adsorption of small molecules on late-transition metal surfaces using these GGA functionals [35]. While PW91 and PBE systematically overestimate the corresponding experimental adsorption energies, RPBE gives more reliable results. In average, the adsorption energies obtained with RPBE are about 20% smaller than those calculated with PW91 and PBE [35].

In Table 2, the calculated values of binding energies (E_B(Au)), atomic charges (q) and spin densities (SD) for the deposition of the Au atom on anionic centers on terrace, edge and corner are presented. Binding energy values show that Au atom adsorbs following the sequence corner(O^{2-}) > edge(O^{2-}) > terrace(O^{2-}). In Fig. 1 the corresponding Au–O distances are reported. Notice that these distances show a decreasing behaviour with: (i) increasing binding energy and (ii) decreasing coordination number of the oxygen atom to which the Au atom is anchored. The Au charge is low and similar for the three cases (about −0.1e). The spin density is concentrated mainly on Au atoms, being somewhat higher on terrace(O^{2-}).

In Table 3, the calculated values of E_B(Au), atomic charges and spin densities for Au atom on F_s sites are summarized. Notice that Au adsorbs more strongly than on anionic centers, being the edge(F_s) the preferred site. It is well known that on F_s centers the charge transfer to the metal atom is substantial, a phenomenon related with the high polarizability of the charge inside the vacancy and the high electron affinity of gold [6–9]. It is interesting to point out how the coordination of Au atom changes on these F_s sites (Fig. 2). It coordinates with four Mg^{2+} on terrace(F_s), with two Mg^{2+} on edge(F_s) and with three Mg^{2+} on corner(F_s). In Fig. 2 the corresponding Au–Mg^{2+} distances are reported. Also in this case these distances show a decreasing behaviour with: (i) increasing binding energy and (ii) decreasing coordination number of the Au atom. In particular, on edge(F_s) the relatively short Au–Mg^{2+} distance can be related to the more contracted electronic cloud around the Au atom (see later) and with the lowest negative charge on Au.

Table 1
Calculated binding energies (Eq. (1)) of adsorbed Au atom on MgO(1 0 0) (terrace sites). Comparison with other reported values.

Terrace(O^{2-})	Terrace(F_s)	Functional/code	References
0.90	3.12	PW91/VASP	[12]
0.89	3.17	PW91/VASP	[7]
0.87	3.04	PBE/PWscf	[13]
0.73	2.93	B3LYP/G03	This work
0.66	2.50	RPBE/DACAPO	[14]

Table 2
Main energetic and electronic population parameters for Au atoms deposited on anionic sites of MgO(1 0 0). Energies are expressed in eV and charges in electron units. SD is the spin density.

	Terrace(O^{2-})	Edge(O^{2-})	Corner(O^{2-})
E_B(Au)	0.73	0.90	1.05
q(Au)	−0.13	−0.14	−0.15
q(O^{2-})	−1.74	−1.71	−1.73
SD(Au)	0.76	0.72	0.72
SD(O^{2-})	0.24	0.24	0.20

Table 3
Main energetic and electronic population parameters for Au atoms deposited on F_s sites of MgO(1 0 0). Energies are expressed in eV and charges in electron units. SD is the spin density.

	Terrace(F_s)	Edge(F_s)	Corner(F_s)
E_B(Au)	2.93	3.14	3.07
q(Au)	−0.88	−0.74	−0.82
SD(Au)	0.44	0.55	0.50

To study the charge distribution after deposition, the charge density difference $\Delta\rho = \rho(Au_1/MgO) - \rho(MgO) - \rho(Au_1)$ was calculated, by subtracting from the total charge density of the Au_1/MgO system the densities of the component fragments, and mapped it on the plane that contains the metal atom (Fig. 3). For terrace(O^{2-}), we can observe a depletion of the charge density on the O anion and a charge accumulation around the Au atom. The lack of accumulation of electron density in the region between the Au atom and the oxide surface indicates that the intraunit polarization of Au atom makes an important contribution to the Au–MgO bonding [7]. For edge(O^{2-}) and corner(O^{2-}) the $\Delta\rho$ maps are similar (not shown).

From the $\Delta\rho$ maps we can see that on terrace(F_s) the electronic density is accumulated surrounding the Au atom including the interface region (Fig. 3b). On edge(F_s) and corner(F_s) the situation is fairly different (Fig. 3c and d). In these cases the electronic density accumulation is toward two nearby cations, forming two lobes. The origin of this particular shape can be understood by an inspection of the HOMO(α) (singly occupied) of the Au_1/MgO systems (Fig. 4). On terrace(F_s) the HOMO(α) presents two lobes, one inward and the other outward the surface (Fig. 4b). On edge(F_s) and corner(F_s) these lobes are orientated in a different way, being exposed outward the surface and extended sideward the Au atom (Fig. 2c and d). Then, the $\Delta\rho$ shape at low-coordinated sites is due to the participation of the corresponding HOMO(α) to the total electron density which contributes to a charge accumulation in these regions.

The results concerning the CO adsorption on Au_1/MgO on O^{2-} sites are reported in Table 4 and Fig. 5. On corner(O^{2-}) site CO adsorbs more strongly with a binding energy of 0.69 eV. For edge(O^{2-}) and terrace(O^{2-}) the corresponding values are 0.52 and 0.51 eV, respectively. Giordano et al. have calculated adsorption energies on terrace(O^{2-}) by means of different methods obtaining a relatively wide range [25]. For example, they found a value of about 0.6 eV (without BSSE correction) using cluster models and B3LYP, i.e., a similar approach than here. At PW91 level in combination with the supercell approximation, they calculated a binding energy of 0.81 eV. Using the unrestricted coupled-cluster singles

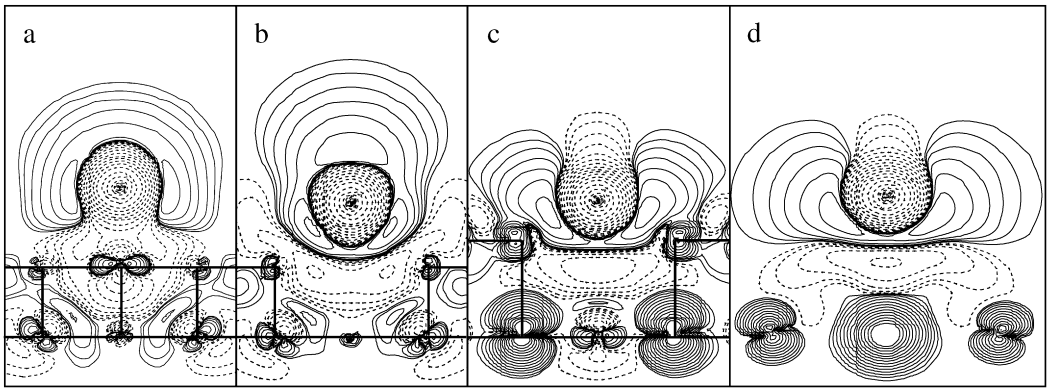

Fig. 3. Charge density difference, $\Delta\rho = \rho(Au_1/MgO) - \rho(MgO) - \rho(Au_1)$, for Au atom deposited on: (a) terrace(O^{2-}); (b) terrace(F_s); (c) edge(F_s); (d) corner(F_s). In c, $\Delta\rho$ is mapped along the [1 1 0] plane. In d, $\Delta\rho$ is mapped along a plane normal to the [1 1 1] plane. Dotted lines correspond to regions with $\Delta\rho < 0$, and solid lines to regions with $\Delta\rho > 0$. Contour levels for mapping are: ±1.0, ±0.5, ±0.25…± 0.00012 a.u.

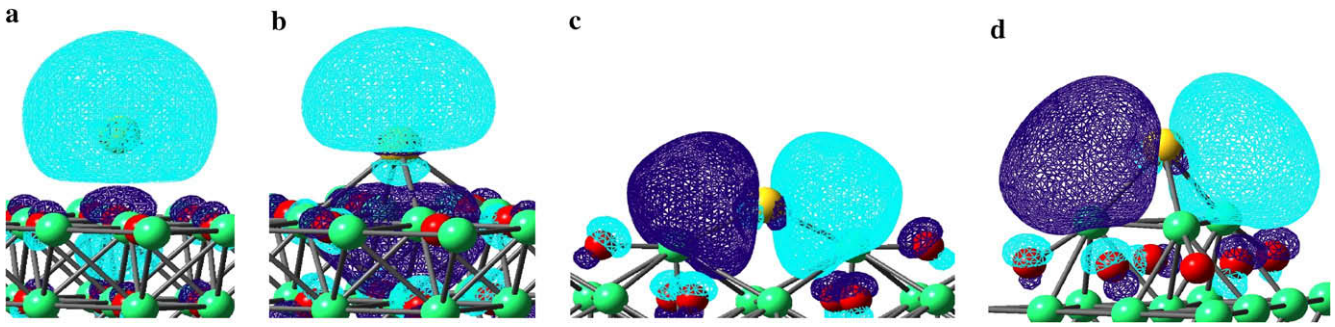

Fig. 4. Schematic representation of the single occupied HOMO(α) of Au atom deposited on: (a) terrace(O^{2-}); (b) terrace(F_s); (c) edge(F_s) and (d) corner(F_s).

Table 4
Main energetic and electronic population parameters for CO adsorbed on Au atoms deposited on anionic sites of MgO(1 0 0). CO stretching frequency (ν) and its shift with respect to free CO ($\Delta\nu$) are also shown. Energies are expressed in eV, charges in electron units and frequencies in cm^{-1}. SD, spin densities; $\Delta\varepsilon$, core level binding energies (CLBE).

	Terrace(O^{2-})	Edge(O^{2-})	Corner(O^{2-})
E_B(CO)	0.51	0.52	0.69
q(Au)	+0.23	+0.26	+0.29
q(C)	+0.20	+0.19	+0.15
q(O)	−0.53	−0.52	−0.56
q(CO)	−0.33	−0.33	−0.41
SD(Au)	0.32	0.29	0.23
SD(C)	0.45	0.44	0.51
SD(O)	0.15	0.14	0.15
$\Delta\varepsilon$(C,1s)	−2.47	−2.17	−3.55
$\Delta\varepsilon$(O,1s)	−3.23	−2.95	−4.33
ν	1871	1897	1845
$\Delta\nu$	−332	−306	−358

and doubles with the perturbative estimate of the triples contribution [CCSD(T)] methodology and the embedded O(Mg-ECP)$_5$ minimal cluster the value is relatively low, 0.35 eV.

On terrace(O^{2-}) the calculated atomic spin densities (SD) are: SD(C) = 0.45, SD(O) = 0.15 and SD(Au) = 0.32. Giordano at al. [25] also found high SD on CO with values varying from 0.6 to 0.8 on CO (and from 0.1 to 0.3 on Au), depending on the computational method. On the other hand, the SD distribution for free AuCO is more concentrated on the Au atom: SD(C) = 0.17, SD(O) = 0.05 and SD(Au) = 0.84, similarly to the data reported by Giordano at al. [25]. These SD distributions are compatible with the appearance of an important electronic charge transfer to CO to yield the Au^+CO^- complex. A complex like that was proposed on MgO(1 0 0) in ref. [11] and could account for the observed red-shift of the CO stretching frequency on Au_1/MgO. The SD distribution on C, O and Au atoms for the edge(O^{2-}) and corner(O^{2-}) sites follow the same trend than for the terrace(O^{2-}) site.

In order to complement the information obtained from SD results and to study the charge distribution from another point of view, NBO atomic charges and CLBE shifts were also computed. The calculated NBO charges for the CO adsorption on Au atoms at O^{2-} sites are shown in Table 4. The total CO charge is −0.33e for terrace(O^{2-}) and edge(O^{2-}), and −0.41e for corner(O^{2-}). Thus, the NBO analysis does not support a so relevant charge transfer from Au to CO as suggested by the SD values. The CLBE values are all negative showing the same direction of charge transfer for CO. Besides, their relative values are in qualitative agreement with NBO charges: the shift is greater on corner(O^{2-}) indicating a large amount of negative charge for CO at this site (for the sake of comparison, the corresponding $\Delta\varepsilon$ values for the isolated CO^- anion are −7.90 eV and −8.23 eV for C(1s) and O(1s), respectively). On the other hand, the AuCO fragment has a total NBO charge in the range −0.07 to −0.12e, becoming only slightly negative charged.

Concerning the CO frequency values, dramatic red-shifts were found on O^{2-} sites between −358 and −306 cm^{-1}, following the sequence: corner(O^{2-}) > terrace(O^{2-}) > edge(O^{2-}). At the corner(O^{2-}) site, the electronic cloud in the Au atom is relatively more polarizable than in the other cases because the first Mg^{2+} neighbours are very distant (the Au–Mg^{2+} distance is 3.724 Å). As a consequence, there is a substantial charge transfer to CO, populating the antibonding $2\pi^*$ orbital and largely shifting the CO stretching frequency. The difference observed between terrace(O^{2-}) and edge(O^{2-}) in the CO frequency values cannot be directly related to the NBO charge of CO because they are similar for both geometries. However, CLBE values seem to indicate a minor CO negative

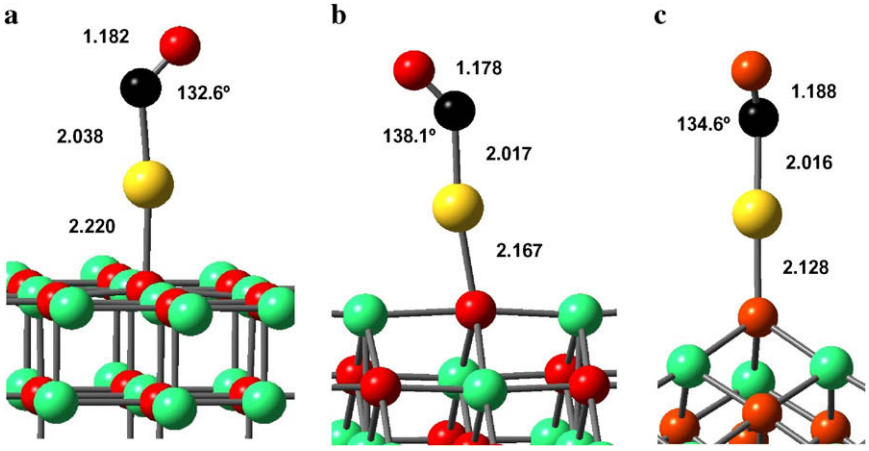

Fig. 5. Schematic representation of CO adsorbed on Au atoms deposited on anionic sites (O^{2-}): (a) terrace; (b) edge; (c) corner. Black spheres: C atoms. The rest of the colour scheme is the same as in Fig. 1. (For interpretation of the references to colour in this figure legend, the reader is referred to the web version of this article.)

charge at edge(O^{2-}). It is likely that the backdonation might be somewhat different in these sites yielding to the observed difference in the CO frequencies.

The CO frequency value of 1871 cm^{-1} obtained here on terrace(O^{2-}) is different than that reported by Sterrer et al., 1910 cm^{-1} [10]. They used a similar embedded technique but a smaller cluster, Mg_9O_9(Mg-ECP)$_{16}$, and a smaller basis set, 6–31G(d). Notice that this behaviour was just outlined in Section 2.

It is interesting to point out that the CO interaction with Au atom at gas phase was recently studied using different DFT functionals and more accurate wave-function based (ab initio) methods [25,36]. The performance of various DFT functionals varies widely being the hybrid B3LYP the one that presents best results, in comparison with those obtained at CCSD(T) level [36]. It was observed that the calculation of the CO frequency is very delicate, because small errors in the Au–C–O angle can result in large errors in the CO frequency. However, this dependence between CO frequency and the tilt angle is not present when the AuCO complex is adsorbed on MgO [25]. In this case the charge transfer to CO leads to a much deeper potential for bending.

We have also performed an analysis on free AuCO at the same level of calculation than for supported Au. The Au–C distance is 2.089 Å, somewhat longer than on MgO at anionic sites. The CO charge is lower than on supported Au, −0.12e. Hence, the CO stretching frequency is shifted by −141 cm^{-1}, a value that is much smaller in magnitude than that for the supported case. So, the dramatic red-shift observed for supported Au on O^{2-} sites is a clear indication of a strong support effect. As we observe in the $\Delta\rho$ maps (Fig. 3a), the MgO surface acts in such a way that the electronic charge is accumulated upward the Au atom, favouring the interaction with the $2\pi^*$ MO of CO.

In Fig. 6 the optimized geometries of CO adsorption on Au atom on F_s are presented. In all cases we started with the CO molecule above the gold as initial geometry. On terrace(F_s) the CO molecule finalizes with a relatively long Au–C distance with the CO interacting rather laterally with Au. Conversely, CO keeps above the Au atom on edge(F_s) and corner(F_s). In these sites the Au–C distance is nearly 0.2 Å shorter and the Au–C–O angle 10–20° greater than on terrace(F_s).

For Au atoms supported on F_s sites, CO adsorbs weakly than on anionic sites (Table 5). Noticeably, NBO charges for CO are not substantially different than on O^{2-} sites. The charge of the AuCO complex (−1.02e for terrace(F_s) and corner(F_s), and −0.92e for edge(F_s)) is somewhat higher than for a single adsorbed Au (−0.88e). Thus, CO induces a little amount of charge transfer from the vacancy to the adsorbed complex. The corresponding CLBE shifts are not so different than those for O^{2-} sites, suggesting a rather similar charge transfer to CO, in agreement with NBO results. The SD is about 0.6–0.7 for the AuCO complex; the rest of it is spread out toward the cavity. It is noteworthy that the SD for the AuCO complex on the regular sites is nearly 0.3 greater, showing a larger localization in these cases. The same observation is obtained if we compare the SDs for the single adsorbed Au atom on regular and defective sites. This should be related to a greater spin pairing of Au and vacancy electrons, in agreement with the larger binding energies for Au atom on F_s sites.

The difference in the geometries between F_s at topological defects and terrace(F_s) can be understood by considering the interaction of the HOMO(α) of the Au/MgO system with the $2\pi^*$ MO of CO. By symmetry, this interaction of bonding character is highly favoured on edge(F_s) and corner(F_s) because the two lobes of this HOMO are exposed outside the surface (Figs. 4c and d and 7c and d). On terrace(F_s) one of the lobes is inward the surface; thus, in this case the overlap is less favoured and the Au–CO interaction is rather lateral (Figs. 4b and 7b). Counteracting this bonding interaction, there is a strongly antibonding interaction produced between the 5σ MO of CO and more internal orbitals of the Au/MgO system, the HOMO-1(α) and the HOMO(β), both spheroidal orbitals centered at the Au atom and with very similar orbital energies (Fig. 7e–g). A very strong Pauli repulsion takes place in this situation. This can explain the relatively weak CO bonding with Au at F_s centers. On the other hand, the interaction of bonding character between the $2\pi^*$ MO and the HOMO(α) of Au_1 on terrace(O^{2-}) is produced by means of only one lobe of $2\pi^*$ MO as it is shown in Fig. 7a. The corresponding pictures for edge(O^{2-}) and corner(O^{2-}) are very similar (not shown). On anionic sites the 5σ MO of CO overlaps with Au orbitals producing a very strong bonding contribution (donation).

In relation with the CO frequency shifts on Au at F_s sites, we can observe that the frequency shift on terrace(F_s) is practically the same that on terrace(O^{2-}). In comparison, Sterrer et al. have found a value which is 28 cm^{-1} lesser than on terrace(F_s) [10]. However, their periodic supercell calculations show a linear AuCO complex, fairly different than the geometry optimized with our cluster approximation (see Fig. 6a).

In comparison with terrace(F_s), the CO frequency shift is less pronounced on edge(F_s) and corner(F_s) sites, with values of −232 and −273 cm^{-1}, respectively. With respect to the terrace(O^{2-}) site these values correspond to blue-shifts of 100 and 59 cm^{-1}, respec-

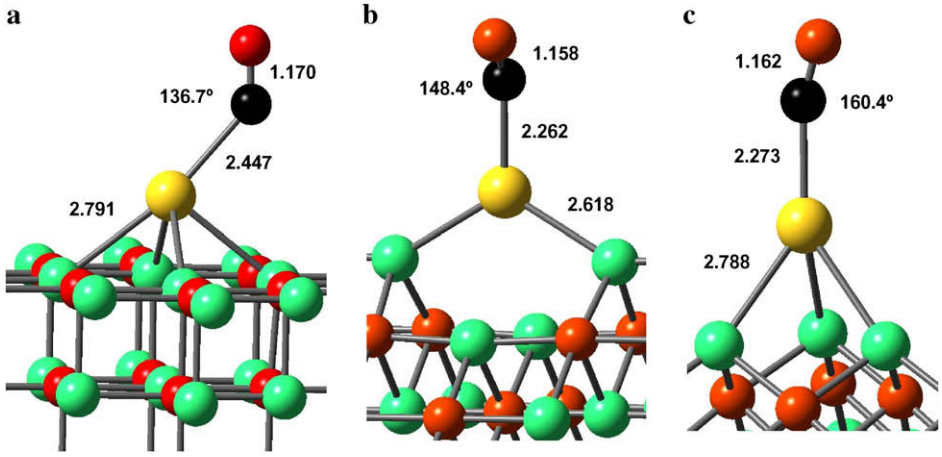

Fig. 6. Schematic representation of CO adsorbed on Au atoms deposited on F_s sites: (a) terrace; (b) edge; (c) corner. Black spheres: C atoms. The rest of the colour scheme is the same as in Fig. 1. (For interpretation of the references to colour in this figure legend, the reader is referred to the web version of this article.)

Table 5
Main energetic and electronic population parameters for CO adsorbed on Au atoms deposited on F_s sites of MgO(1 0 0). CO stretching frequency (ν) and its shift with respect to free CO ($\Delta\nu$) are also shown. Energies are expressed in eV, charges in electron units and frequencies in cm−1. SD, spin densities; $\Delta\varepsilon$, core level binding energies (CLBE).

	Terrace(F_s)	Edge(F_s)	Corner(F_s)
E_B(CO)	0.14	0.25	0.26
q(Au)	−0.65	−0.59	−0.65
q(C)	+0.18	+0.19	+0.16
q(O)	−0.55	−0.52	−0.53
q(CO)	−0.37	−0.33	−0.37
SD(Au)	0.29	0.40	0.39
SD(C)	0.26	0.23	0.30
SD(O)	0.09	0.05	0.05
$\Delta\varepsilon$ (C,1s)	−3.09	−1.97	−2.76
$\Delta\varepsilon$ (O,1s)	−3.46	−2.39	−3.15
ν	1873	1971	1930
$\Delta\nu$	−330	−232	−273

tively, in line with the shift of 70 cm^{-1} observed by IR spectroscopy on defective and perfect MgO(1 0 0) surface [10]. As above commented, at edge(F_s) and corner(F_s) sites, the CO molecule overlaps efficiently with Au by means of the $2\pi^*$ MO. When CO vibrates, it does against a region with a high electron density which acts to "stiffen" the motion of the C atom. This effect is usually known as "wall effect" which by itself contributes to change the CO frequency to higher values [37,38]. As a consequence, the red-shift is lower on F_s at low-coordinated sites than on terrace(O^{2-}) as suggested by experimental measurements. On the other hand, on terrace(F_s), the Au–C distance is relatively long and CO is oriented in such a way that it does not vibrate directly against the charged Au atom. In this case the wall effect is therefore relatively poor and the corresponding frequency strongly red-shifted.

Moreover, it is pertinent to interpret why the red-shift on edge(F_s) is lower than on corner(F_s) (−232 vs. −273 cm^{-1}). As it was already mentioned, the Au atom on edge(F_s) has a lower neg-

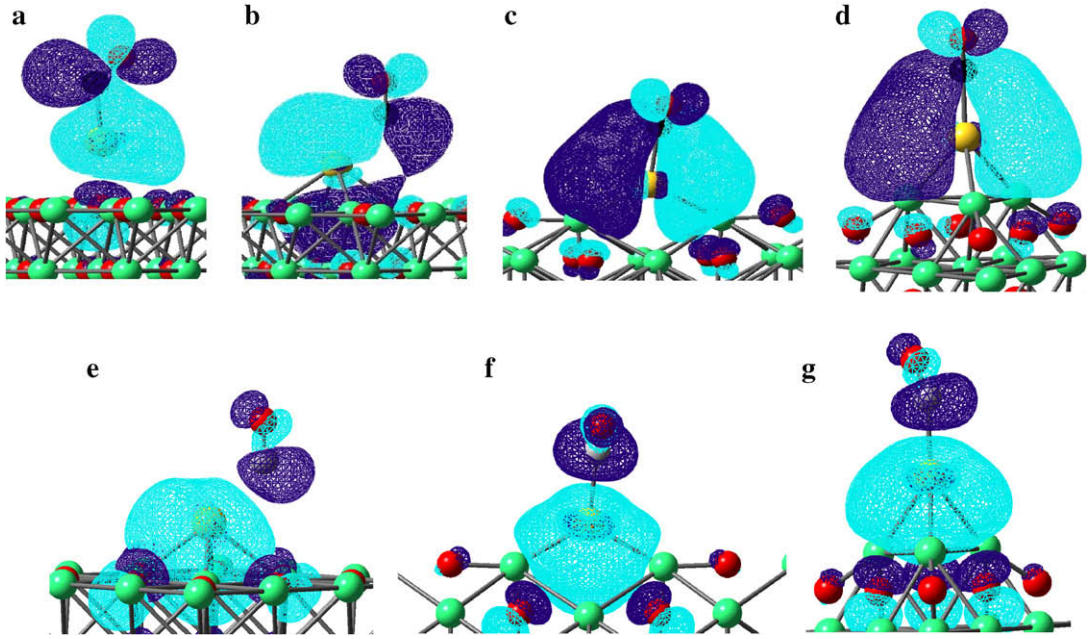

Fig. 7. (a–d): Schematic representation of the single occupied HOMO(α) of CO adsorbed on supported Au. (a) Terrace(O^{2-}); (b) terrace(F_s); (c) edge(F_s); (d) corner(F_s). These MOs are produced from the interaction between the $2\pi^*$ MO of CO and the HOMO(α) of Au/MgO (see Fig. 4). (e–g): Antibonding interaction between the 5σ MO of CO and the HOMO-1(α) (or HOMO(β)) of Au/MgO. (e) Terrace(F_s); (f) edge(F_s); (g) corner(F_s).

ative charge and furthermore it is less diffuse than on corner(F_s). In consequence, the backdonation to $2\pi^*$ is relatively low, a fact that is reflected on the smaller negative charge on CO and the lesser CLBE shift. As a result, the C–O distance is shorter on edge(F_s) and lower the red-shift.

Finally, it is very interesting to compare the present results of CO adsorption on Au_1/MgO(terrace) with those corresponding to NO (a molecule with an additional electron than CO) [9]. The adsorption of NO is stronger than CO; the binding energies for NO are −1.08 and −0.49 eV on gold atoms deposited on O^{2-} and F_s sites, respectively. The greater binding energy can be interpreted in terms of the spin density distribution at the metallic site: NO is a radical with an unpaired electron mainly located on the N atom and it can couple strongly with other species with an unpaired electron such as MgO-supported Au_1. The NO charge on Au/terrace(O^{2-}) is −0.37e, i.e., similar than for CO on this same site. However, it is higher on Au/terrace(F_s): −0.57e. This charge populates the antibonding $2\pi^*$ MO of NO producing a remarkable red-shift of 397 cm^{-1}. On the other hand, on terrace(O^{2-}) this shift is −336 cm^{-1}.

An interesting question to be answered is if the "wall effect" is also present for NO at low coordination sites. On Au atoms deposited on O^{2-} at terrace, edge and corner sites, the NO frequency shift varies in the range of −330 and −360 cm^{-1} [39]. On the other hand, for a Au atom supported on F_s at these same sites the NO frequency shift varies between −400 and −440 cm^{-1}. For NO the bonding/backbonding mechanism involves only the $2\pi^*$ MO with a relatively poor participation of 5σ [9,40]. Hence, in this case the shifts are those that one intuitively would expect if only changes at the $2\pi^*$ MO populations are taken into account.

4. Conclusions

CO adsorbs on atomic Au deposited on anionic (O^{2-}) sites following the sequence: corner > edge ≈ terrace, with binding energies varying in the range of 0.51–0.69 eV. On neutral oxygen vacancies (F_s centers) the adsorption is weaker (0.14–0.26 eV). The calculated NBO charges support the existence of the $Au^{\delta+}CO^{\delta-}$ complex on the anionic site. Interestingly, on F_s the predicted CO charge is not very different than on O^{2-}; it changes from about −0.3 to −0.4e for all the sites.

Concerning the CO frequency values, dramatic red-shifts were found on O^{2-} sites. The calculated shifts are: −358, −332 and −306 cm^{-1} for corner, terrace and edge, respectively. At corner site, the electronic cloud on the Au atom is relatively more diffuse than on the other cases because the first Mg^{2+} neighbours are very distant. In consequence, there is a higher charge transfer to CO with the corresponding larger red-shift.

On terrace(F_s), the red-shift is very similar than on terrace(O^{2-}). However, the red-shift is less pronounced on edge(F_s) and corner(F_s): −232 and −273 cm^{-1}, respectively. The available experimental measurements indicate that Au adsorbs on terrace at perfect MgO(1 0 0) and at topological defects on O-deficient surfaces. Upon CO adsorption, the observed IR features on defective surface is blue-shifted by 70 cm^{-1} with respect to the perfect surface. Our calculations predicted blue-shifts by 100 and 59 cm^{-1} at edge(F_s) and corner(F_s), respectively. These results are rather unexpected because following the generally accepted scheme the shifts at F_s should be larger owing to the expected negative charge on Au at these sites.

A molecular-orbital-based reasoning suggests the following picture. On terrace(F_s) the HOMO(α), mainly centered on Au, presents two lobes: one inward and the other outward the surface. On edge(F_s) and corner(F_s) these lobes are orientated in a different way, being exposed outward the surface and extended sideward the Au atom. By symmetry, the interaction of the $2\pi^*$ MO of CO is highly favoured on F_s at low-coordinated sites. In fact, the Au–C distance is 0.2 Å shorter than on terrace(F_s). When CO vibrates, it does against a region with a high electron density which acts to "stiffen" the motion of the C atom. This is the so-called "wall effect" which contributes to change the CO frequency to higher values. As a consequence, the red-shift is lower on F_s at low-coordinated sites than on terrace(O^{2-}), as indicated by experimental measurements.

Acknowledgments

The authors acknowledge the financial support of Universidad Nacional del Sur, CONICET and ANPCyT of Argentina.

References

[1] U. Heiz, W.D. Schneider, J. Phys. D: Appl. Phys. 33 (2000) R85.
[2] Z. Yang, S. Chinta, A.A. Mohamed, J.P. Fackler, D.W. Goodman, J. Am. Chem. Soc. 127 (2005) 1604.
[3] M. Frank, M. Bäumer, R. Kuehnemuth, H.-J. Freund, J. Phys. Chem. B 105 (2001) 8569.
[4] G.C. Bond, C. Louis, D.T. Thompson, Catalysis by Gold, Imperial College Press, London, 2006.
[5] D. Scarano, S. Bordiga, C. Lamberti, G. Spoto, G. Ricchiardi, A. Zecchina, C. Otero Areán, Surf. Sci. 411 (1998) 272.
[6] M. Sterrer, M. Yulikov, E. Fischbach, M. Heyde, H. Rust, G. Pacchioni, T. Risse, H.-J. Freund, Angew. Chem. Int. Ed. 45 (2006) 2630.
[7] A. Del Vitto, G. Pacchioni, F. Delbecq, P. Sautet, J. Phys. Chem. B 109 (2005) 8040.
[8] C. Inntam, L.V. Moskaleva, K.M. Neyman, V.A. Nasluzov, N. Rösch, Appl. Phys. A 82 (2006) 181.
[9] S.A. Fuente, P.G. Belelli, R.M. Ferullo, N.J. Castellani, Surf. Sci. 602 (2008) 1669.
[10] M. Sterrer, M. Yulikov, T. Risse, H.J. Freund, J. Carrasco, F. Illas, C. Di Valentin, L. Giordano, G. Pacchioni, Angew. Chem. Int. Ed. 45 (2006) 2633.
[11] L. Giordano, U. Martinez, S. Sicolo, G. Pacchioni, J. Chem. Phys. 127 (2007) 144713.
[12] A. Bogicevic, D.R. Jennison, Surf. Sci. 515 (2002) L481.
[13] G. Barcaro, A. Fortunelli, J. Chem. Theory Comput. 1 (2005) 972.
[14] P. Frondelius, H. Häkkinen, K. Honkala, New J. Phys. 9 (2007) 339.
[15] Z. Yang, R. Wu, Q. Zhang, D.W. Goodman, Phys. Rev. B 65 (2002) 155407.
[16] L.M. Molina, J.A. Alonso, J. Phys. Chem. C 111 (2007) 6668.
[17] C. Di Valentin, A. Scagnelli, G. Pacchioni, T. Risse, H.-J. Freund, Surf. Sci. 600 (2006) 2434.
[18] S. Dahl, A. Logadottir, R.C. Egeberg, J.H. Larsen, I. Chorkendorff, E. Törnqvist, J.K. Nørskov, Phys. Rev. Lett. 83 (1999) 1814.
[19] M.M. Branda, C. Di Valentin, G. Pacchioni, J. Phys. Chem. B 108 (2004) 4752.
[20] C. Di Valentin, R.M. Ferullo, R. Binda, G. Pacchioni, Surf. Sci. 600 (2006) 1147.
[21] A.D. Becke, J. Chem. Phys. 98 (1993) 5648.
[22] M.J. Frisch et al., Gaussian 03, Revision C.02, Gaussian Inc., Wallingford, CT, 2004.
[23] J. Carrasco, C. Sousa, F. Illas, P.V. Sushko, A.L. Shluger, J. Chem. Phys. 125 (2006) 074710.
[24] J. Carrasco, N. Lopez, F. Illas, H.-J. Freund, J. Chem. Phys. 125 (2006) 074711.
[25] L. Giordano, J. Carrasco, C. Di Valentin, F. Illas, G. Pacchioni, J. Chem. Phys. 124 (2006) 174709.
[26] P.J. Hay, W.R. Wadt, J. Chem. Phys. 82 (1985) 270.
[27] P.J. Hay, W.R. Wadt, J. Chem. Phys. 82 (1985) 299.
[28] I. Yudanov, G. Pacchioni, K. Neyman, N. Rösch, J. Phys. Chem. B 101 (1997) 2786.
[29] S.F. Boys, F. Bernardi, Mol. Phys. 19 (1970) 553.
[30] A.E. Reed, L.A. Curtiss, F. Weinhold, Chem. Rev. 88 (1988) 899.
[31] A. Citra, X. Wang, L. Andrews, J. Phys. Chem. A 106 (2002) 3287.
[32] S. Lizzit, A. Baraldi, A. Grosso, K. Reuter, M.V. Ganduglia-Pirovano, C. Stampfl, M. Scheffler, M. Stichler, C. Keller, W. Wurth, D. Menzel, Phys. Rev. B 63 (2001) 205419.
[33] J.P. Perdew, J.A. Chevary, S.H. Vosko, K.A. Jackson, M.R. Pederson, D.J. Singh, C. Fiolhais, Phys. Rev. B 46 (1992) 6671.
[34] J.P. Perdew, K. Burke, M. Ernzerhof, Phys. Rev. Lett. 77 (1996) 3865.
[35] B. Hammer, L.B. Hansen, J.K. Nørskov, Phys. Rev. B 59 (1999) 7413.
[36] P. Schwerdtfeger, M. Lein, R.P. Krawczyk, C.R. Jacob, J. Chem. Phys. 128 (2008) 124302.
[37] P.S. Bagus, W. Müller, Chem. Phys. Lett. 115 (1985) 540.
[38] D. Curulla, A. Clotet, J.M. Ricart, F. Illas, J. Phys. Chem. B 103 (1999) 5246.
[39] Unpublished results.
[40] X. Ding, Z. Li, J. Yang, J.G. Hou, Q. Zhu, J. Chem. Phys. 121 (2004) 2558.